Physics in Medicine & Biology

FAST TRACK COMMUNICATION • OPEN ACCESS

3D ultrafast ultrasound imaging *in vivo*

To cite this article: Jean Provost *et al* 2014 *Phys. Med. Biol.* **59** L1

OPEN ACCESS
IOP Publishing | Institute of Physics and Engineering in Medicine
Fast Track Communications
Physics in Medicine & Biology
Phys. Med. Biol. **59** (2014) L1–L13
doi:10.1088/0031-9155/59/19/L1

Fast Track Communication

3D ultrafast ultrasound imaging *in vivo*

Jean Provost, Clement Papadacci, Juan Esteban Arango, Marion Imbault, Mathias Fink, Jean-Luc Gennisson, Mickael Tanter[1] and Mathieu Pernot[1]

ESPCI ParisTech, PSL Research University, Institut Langevin, 1 rue Jussieu, F-75005, Paris, France
CNRS, UMR 7587 Institut Langevin, 1 rue Jussieu, F-75005, Paris, France
INSERM, U979 Institut Langevin, 1 rue Jussieu, F-75005, Paris, France
Université Paris Diderot, Sorbonne Paris Cité, Institut Langevin, UMR 7587, 1 rue Jussieu, F-75005, Paris, France
Sorbonne Universités, UPMC Univ Paris 06, UMR 7587, Institut Langevin, 1 rue Jussieu, F-75005, Paris, France
[1] MP and MT are co-last authors

E-mail: Mathieu.pernot@espci.fr

Received 19 June 2014, revised 24 July 2014
Accepted for publication 12 August 2014
Published 10 September 2014

Abstract

Very high frame rate ultrasound imaging has recently allowed for the extension of the applications of echography to new fields of study such as the functional imaging of the brain, cardiac electrophysiology, and the quantitative imaging of the intrinsic mechanical properties of tumors, to name a few, non-invasively and in real time. In this study, we present the first implementation of Ultrafast Ultrasound Imaging in 3D based on the use of either diverging or plane waves emanating from a sparse virtual array located behind the probe. It achieves high contrast and resolution while maintaining imaging rates of thousands of volumes per second. A customized portable ultrasound system was developed to sample 1024 independent channels and to drive a 32 × 32 matrix-array probe. Its ability to track in 3D transient phenomena occurring in the millisecond range within a single ultrafast acquisition was demonstrated for 3D Shear-Wave Imaging, 3D Ultrafast Doppler Imaging, and, finally, 3D Ultrafast combined Tissue and Flow Doppler Imaging. The propagation of shear waves was tracked in a phantom and used to characterize its stiffness. 3D Ultrafast Doppler was used to obtain 3D maps of Pulsed Doppler, Color Doppler, and Power Doppler quantities in a single acquisition and revealed, at thousands of volumes per second, the complex 3D flow patterns occurring in the ventricles of the human heart during an entire cardiac cycle, as well

as the 3D *in vivo* interaction of blood flow and wall motion during the pulse wave in the carotid at the bifurcation. This study demonstrates the potential of 3D Ultrafast Ultrasound Imaging for the 3D mapping of stiffness, tissue motion, and flow in humans *in vivo* and promises new clinical applications of ultrasound with reduced intra—and inter-observer variability.

Keywords: ultrasound imaging, ultrafast imaging, 3D ultrasound imaging, volumetric imaging, blood flow, tissue Doppler, cardiac imaging

S Online supplementary data available from stacks.iop.org/PMB/59/00L1/mmedia

(Some figures may appear in colour only in the online journal)

Over the last few years, 2D ultrasound imaging has undergone important technical improvements with the advent of software-based systems that enable the implementation of ultrahigh frame rate imaging techniques: up to 20 000 frames s^{-1} are achieved, as opposed to the 50–200 frames s^{-1} used in traditional clinical systems. When such high frame rates are achieved in a large field of view, e.g. by using either plane wave ultrasound transmissions (Sandrin *et al* 1999, Tanter *et al* 2002), diverging wave transmissions (Couade *et al* 2009, Honjo *et al* 2010, Provost *et al* 2011b, Papadacci *et al* 2014a) or gating techniques (Pernot *et al* 2007, Wang *et al* 2008, Provost *et al* 2010), they allow for the study of rapid phenomena, such as the propagation of artificially-induced shear waves (Sandrin *et al* 2003, Bercoff *et al* 2004) and natural waves in tissues, e.g. the electromechanical wave in the heart (Provost *et al* 2011a) and the pulse wave in the blood vessels (Fujikura *et al* 2007, Couade *et al* 2010, Konofagou *et al* 2011). For this reason, it corresponds to one of the three categories of wave interactions in the field of multi-wave imaging (Fink and Tanter 2010). Moreover, such high frame rates improve temporal resolution, which in turn provides high-quality tissue motion mapping and blood flow mapping. For example, estimating the heart tissue motion above 500 frames s^{-1} results in a five-fold improvement of the elastographic signal-to-noise ratio (Provost *et al* 2012), while the increase in field-of-view and sensitivity of Ultrafast Doppler Imaging provides full-view cardiac blood flow maps and images of blood vessels with unprecedented resolution (Mace *et al* 2011, Demené *et al* 2014). These new techniques have bred entirely new fields of clinical applications for ultrasound imaging (Tanter and Fink 2014), such as the quantitative characterization of tumors (Tanter *et al* 2008), functional imaging of the brain (Macé *et al* 2011, Osmanski *et al* 2014), non-invasive imaging of cardiac electrophysiology (Provost *et al* 2013), the study of the arterial stiffness in hypertension (Vappou *et al* 2010), and high resolution vector flow imaging (Udesen *et al* 2008, Dort *et al* 2012, Ekroll *et al* 2013, Yiu *et al* 2014), to name a few.

Applying these techniques in 3D would significantly broaden their scope of application. For example, both shear and natural wave propagation occur in 3D but their quantitative assessment can only be done in 2D at the cost of simplifying assumptions. This aspect is crucially important when attempting to identify a pacing site in the heart for the treatment of arrhythmias (Provost *et al* 2013) or to detect the presence of mechanical anisotropy (Lee *et al* 2012). Moreover, generalizing Ultrafast Doppler Imaging to 3D would allow for new fields of study to emerge such as, e.g. the quantitative, fully non-invasive angiography of complex networks of blood vessels and the imaging of the cardiac fiber orientation (Papadacci *et al* 2014b). Unfortunately, existing commercial 3D ultrasound systems typically rely on hardware-based focused ultrasound beams and thus limited to a few tens of volumes per second. Although many approaches have been proposed in the literature to perform high volume rate volumetric ultrasound imaging (Perrin

et al 2012, Denarie *et al* 2013, Skaug *et al* 2013), none, to our knowledge, provides sufficiently high volume rates to perform motion and blood flow measurement in an entire volume.

The concept of 3D ultrafast imaging at thousands of volumes per second relies on the transmission of a small number of ultrasound defocussed waves that insonify the entire volume of interest. Dynamic focusing is performed in receive whereas, in transmit, the coherent synthetic summation of the ultrasonic volume acquired for each transmission allows for the restoration of a dynamic focus without compromising the ultrafast volume rate. Montaldo *et al* applied this concept in 2D with plane wave transmissions, which resulted in coherent plane wave compounding (Montaldo *et al* 2009) and can be used for the simultaneous mapping of both flow and tissue velocities (Ekroll *et al* 2013) Recently, in the framework of ultrafast imaging of the human heart, we demonstrated the feasibility of compounding diverging waves using a sparse virtual array located behind the probe to achieve high frame rates and large signal-to-noise ratios in 2D *in vivo* at a limited cost in terms of resolution and contrast when compared to standard, low-frame-rate, focused imaging (Papadacci *et al* 2014a). Building on previous theoretical studies of sparse virtual arrays (Lockwood *et al* 1998, Hazard and Lockwood 1999, Nikolov 2001, Nikolov *et al* 2010), we report herein on the development of 3D Ultrafast Ultrasound Imaging based on the emission of diverging or plane waves emanating from virtual sources located behind a 2D-array ultrasound probe. By coherently compounding multiple emissions and by sampling the data of 1024 piezoelectric elements, we demonstrate that it is possible to perform 3D ultrasound imaging at thousands of volumes per second with large contrast and high resolution, in humans *in vivo*.

In this work, we introduce 3D Ultrafast Ultrasound Imaging and showcase potential clinical applications for cardiovascular imaging. More specifically, we describe the system architecture, validate the increase in contrast and resolution associated with coherently compounded emissions, and show the feasibility of motion estimation for shear-wave imaging in phantoms, of blood flow mapping in a full 3D field of view of the human heart, and of the simultaneous 3D mapping of both tissue and blood flow in the carotid artery near the bifurcation during the pulse wave propagation *in vivo* in humans.

1. Methods

1.1. System infrastructure

A customized, programmable, 1024-channel ultrasound system was designed to drive a 32-by-35 matrix array centered at 3 MHz with a 50% bandwidth at −3 dB and a 0.3 mm pitch (Vermon, Tours, France). The 9th, 17th and 25th lines were not connected, resulting in a total number of active elements equal to 1024. The 1024 independent channels could be used simultaneously in transmission, whereas receive channels were multiplexed to 1 of 2 transducer elements. Therefore, each emission was repeated twice, with the first half of the elements receiving during the first emission, and the second half of the elements receiving during the second emission.

All of the data processing, such as delay-and-sum volume beamforming and flow and motion mapping were performed on graphic processing units (K6000, Nvidia, Santa Clara, CA) in a Matlab environment (2013b, Mathworks, Cambridge, MA). Real-time bi-plane beamforming was also implemented for positioning, while volume beamforming was performed in postprocessing at a rate of, typically, a few volumes per second; the reconstruction rate decreased with the imaging depth, the number of compounded emissions, and the reconstruction sampling rate. 3D rendering was performed using Amira software (Visualization Sciences Group, Burlington, MA).

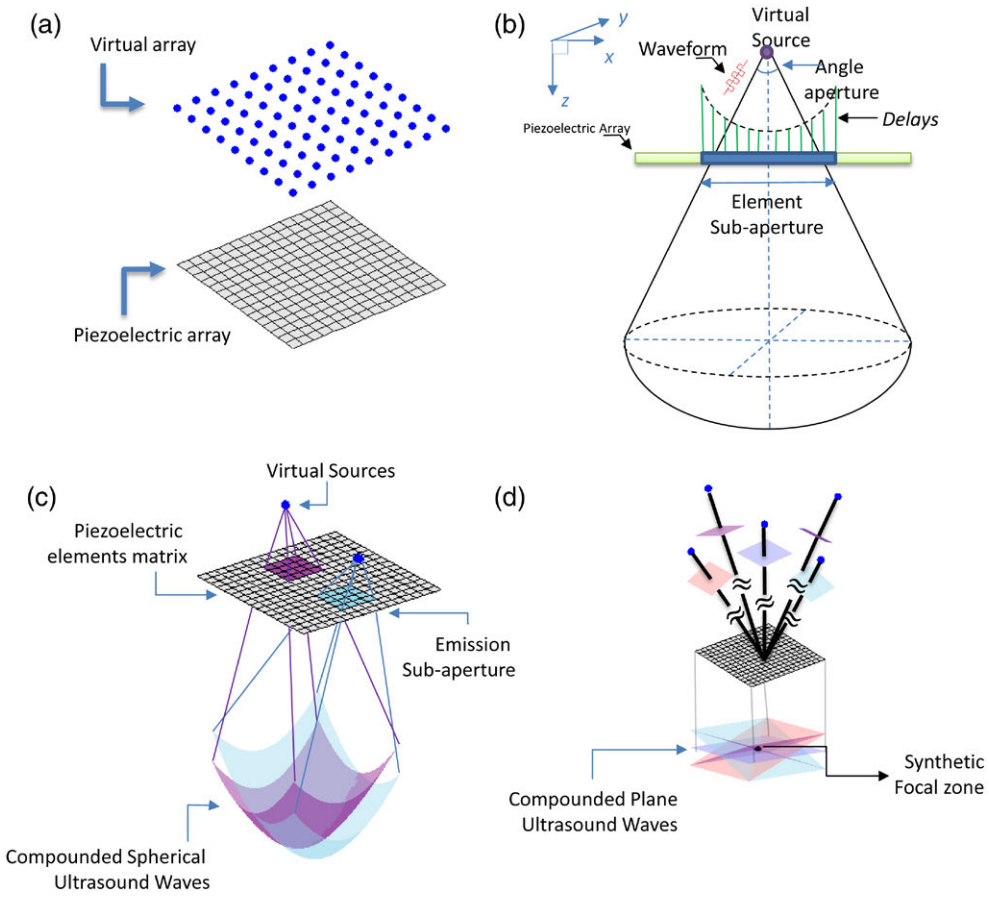

Figure 1. 3D ultrafast ultrasound imaging framework. (*a*) Acquisitions are defined by a virtual array located behind the probe, which is then used to synthetically form an entire imaging volume. (*b*) For each individual source, delays are computed and a sub-aperture is defined. (*c*) When virtual sources are located near the physical probe, the sub-aperture used is smaller and the curvature of the emitted waveform is increased, which results in the insonification of a large field-of-view at the cost of a lower propagated energy. (*d*) When sources are located far behind the probe, larger sub apertures result in larger emitted energy, at the cost of a smaller field of view. In the extreme case of sources located at infinity behind the probe, tilted plane waves are obtained.

1.2. Image formation

A single framework consisting of virtual sources positioned behind the probe was used for compounding emissions (figure 1). More specifically, synthetic beamforming was performed using virtual sources forming a virtual array located behind the probe (figure 1(*a*)). For each source, a physical subaperture and a set of delays were computed (figure 1(*b*)). Emissions from individual sources were performed sequentially, and the radio-frequency data was recorded for each element of the entire physical probe. Volumes were beamformed using delay-and-sum algorithms for each virtual source and subsequently coherently compounded to form a final, high quality volume. Virtual arrays can be tailored to adjust resolution, contrast, signal-to-noise ratio, volume rate, and the field of view in a quasi-continuous

fashion, therefore allowing for the selection of the optimal imaging sequence for a specific application (Lockwood *et al* 1998, Nikolov 2001, Montaldo *et al* 2009, Nikolov *et al* 2010, Papadacci *et al* 2014a).

Indeed, a number of trade-offs between contrast, resolution, volume rate, and field of view exist. For example, as the number of sources is increased, the contrast and resolution improve but the volume rate decreases, and as the distance of the virtual array decreases, the field of view increases but the contrast decreases. More specifically, positioning virtual sources onto the probe itself is equivalent to standard synthetic beamforming, with a high resolution and large field of view, but resulting in a poor volume rate and signal-to-noise ratio at larger depths. As the virtual array is moved behind the probe (figure 1(*c*)), additional physical elements can be recruited to contribute to one emission (i.e. the subaperture) and therefore increased energy is propagated into the tissue and larger signal-to-noise ratios are obtained (Lockwood *et al* 1998). The volume rate can also be adjusted by either increasing the pitch or decreasing the aperture of the virtual array up to the extreme case of using a single source (Provost *et al* 2011b), which is useful for applications requiring very high volume rates such as Ultrafast Doppler Imaging or Shear-Wave Imaging. Placing sources farther behind the probe leads to larger emission subapertures and a smaller field of view. Indeed, a virtual array at infinity (or very far, e.g. at 60 000 mm in this study) results in the emission of plane waves (figure 1(*d*)) with an imaging field of view corresponding to the 2D aperture of the physical probe.

Blood flow and motion estimation were performed by generalizing standard methods reported in previous studies. Namely, the Kasai algorithm (Kasai *et al* 1985) was used to estimate motion in phantoms and in tissues with a half-wavelength spatial sampling. Blood flow was estimated by first applying a high-pass filter to the baseband data and then, for each individual voxel; Power Doppler was obtained by integrating the power-spectral density; Pulsed Doppler was obtained by computing the short-time Fourier transform; and Color Doppler maps were obtained by estimating the first moment of the voxel-specific Pulsed-Doppler spectrogram (Osmanski *et al* 2014).

1.3. Experimental setup

Improvement in resolution was quantified as a function of the number of elements in the virtual array using a customized resolution phantom consisting of 1 mm metallic beads embedded in gelatin. This phantom contained a single layer containing 25 beads and was imaged at 5 different depths to generate a synthetic resolution phantom. Resolution was quantified by measuring the width at −3 dB of the main lobes for each bead. Contrast was quantified in a heart-mimicking phantom (067, CIRS, VA) by calculating the tissue-to-cavity B-mode amplitude ratio in at least 100 and at most 200 voxels at a given depth as a function of the number of sources, as well as in the common carotid of a healthy volunteer near the bifurcation. Shear-Wave Imaging was performed using two probes: the 2D matrix array was used to track the propagation of the shear wave in a 1.92 kPa phantom (acrylamide/bisacrylamide: 5%/0.05% w/w), whereas a standard 6 MHz, 1D linear array (L10-2, Supersonic Imaging, Aix-en-Provence, France), located approximately 2 cm away from the 2D array, generated three 100 μs radiation force 'pushes' approximately 2 cm away from the center of the 2D matrix array. The three push focal zones generated a Mach cone and thus an approximately conical shear wave. Note that the system could be used with the matrix array as a single probe to generate radiation force and to perform ultrafast imaging, but the experiment was not conducted in this study in order to avoid potentially damaging our customized probe. 3D Ultrafast Doppler Imaging was demonstrated by imaging the heart of a normal subject,

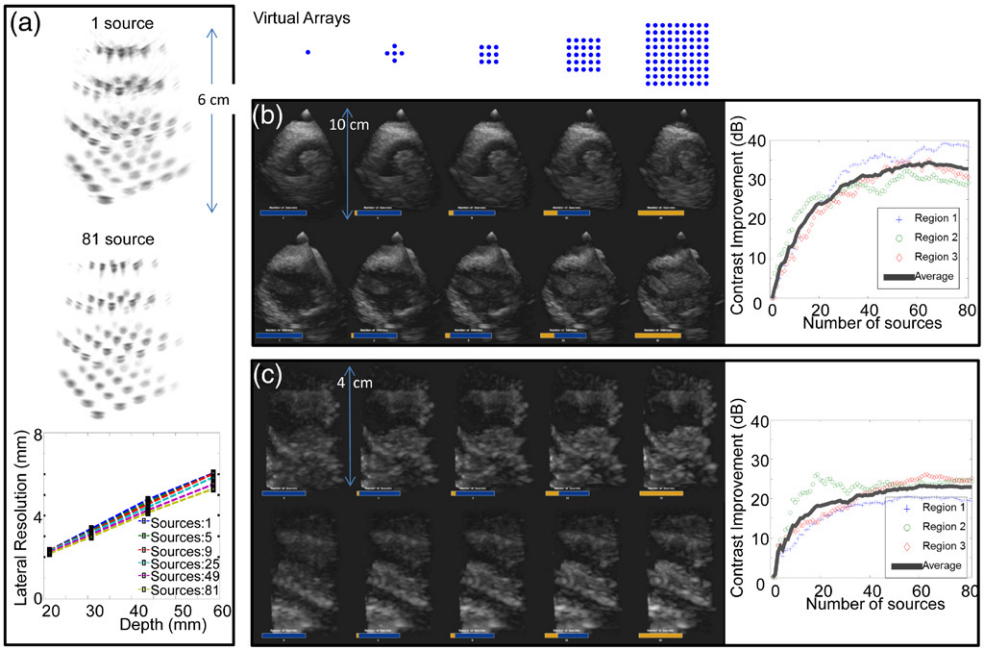

Figure 2. Resolution and contrast. (*a*) An improvement in resolution is obtained when a larger virtual array is used. Indeed, as the number of virtual sources increases, the focal spot narrows and converges toward the optimal case of a focused emission in transmit and receive. Note that transmit–receive dynamic focusing does not lead to a large improvement of the resolution compared to receive only focusing. The improvement in terms of contrast is more important; even a small number of emissions can significantly increase the contrast both in phantoms (*b*) and in the carotid of a human subject *in vivo* (*c*). (*b*) Images of the heart-mimicking phantom in a view approximately aligned with a standard short-axis view (top) and a parasternal long-axis view (bottom). (*c*) Images of the carotid in cross-sectional and longitudinal views (top and bottom, respectively).

and the feasibility of simultaneous 3D Ultrafast Doppler Imaging and 3D Tissue Doppler Imaging was shown through the observation of the propagation of the pulse wave in the carotid artery undergoing pulsatile flow.

2. Results

2.1. Resolution and contrast

Figure 2(*a*) shows the resolution phantom imaged using 1 and 81 virtual sources, respectively, at a 6 cm depth. One can observe an improvement in lateral resolution as the number of sources increased. Interestingly, however, as 3D focusing was performed at every voxel in receive, the resolution remained high, even when using a single emission.

In terms of contrast, however, the situation was different: figure 2(*b*) (supplementary video 1 (stacks.iop.org/PMB/59/00L1/mmedia)) shows the improvement in contrast between the cavity and the tissue in a heart-mimicking phantom for varying depths as the number of coherently-compounded sources increased. The virtual array used had a pitch of 0.53 mm

and a subaperture of 16 × 16 physical elements, and the imaging depth was 10 cm. Sources were added from the center as shown in figure 2. We can observe, as was the case in 2D (Papadacci *et al* 2014a), a rapid increase in contrast with the number of sources. Indeed, the first 10 dB increase in contrast could be obtained using 5 sources instead of one. To obtain a 20 dB increase, 9 sources had to be added, for a total of 16. A plateau was reached near the 30 dB mark, when 36 or more sources were used.

Similar results were obtained *in vivo*. Figure 2(*c*) shows the contrast improvement associated with the use of multiple virtual sources in the carotid of a normal subject *in vivo*. The 9 × 9 virtual array used was positioned at infinity behind the probe to generate plane waves angulated from −8 to 8 degrees with an imaging depth of 4 cm. A similar behavior was observed: a rapid increase in contrast occurred for the first few sources added before reaching a plateau. Notably, the plateau obtained corresponded to a smaller increase in contrast when compared against the phantom experiment of figure 2(*a*) and occurred at approximately 16 sources. This was, however, expected, as the motion of the tissue and blood, along with the hand motion of the sonographer, reduced the contrast enhancing properties of coherent compounding, especially when using a large virtual array requiring long acquisition times (8.4 ms for 81 sources with a 4 cm depth, i.e. 118 volumes s^{-1}).

2.2. 3D Shear-Wave Imaging

3D Shear-Wave Imaging was performed using one virtual source located 2 cm behind the probe and a subaperture corresponding to the entire physical aperture at a rate of 3000 volumes s^{-1} with an imaging depth of 4 cm. Figure 3 (supplementary video 2 (stacks.iop.org/PMB/59/00L1/mmedia)) shows the propagation of the shear wave over a 3 cm distance from three different angles, i.e. from an approximately isometric view (figure 3(*a*)), from the top (figure 3(*b*)), and from the side (figure 3(*c*)). Its velocity was found to be approximately 0.8 m s^{-1}, in accordance with the stiffness of the phantom used (Young's Modulus equal to 1.92 kPa).

2.3. 3D Ultrafast Doppler imaging

Blood flow estimation was performed in the apical view of the heart of a healthy volunteer at 2325 volumes s^{-1} and using a one-source acquisition with an imaging depth of 12 cm. A single ultrafast acquisition allowed the computation, in post-processing, of Color Doppler for each voxel of the volume. Color Doppler maps in which the Power Doppler data was used as a mask to perform the automatic 3D segmentation of the ventricles are shown in figure 4 (supplementary video 3 (stacks.iop.org/PMB/59/00L1/mmedia)). The Color Doppler ciné-loops in multiple complementary views and describing the different phases of the cardiac cycle in the left ventricle are shown: pre-ejection, ejection, rapid filling, diastasis, and atrial systole.

Finally, figure 5 (supplementary video 4 (stacks.iop.org/PMB/59/00L1/mmedia)) demonstrates how the high-quality acquisition using 81 sources can be used to display 1) the anatomy using a compounded B-mode, and combined to a one-source acquisition to quantify 2) Blood flow using Ultrafast Doppler Imaging and 3) motion of the carotid walls using Tissue Doppler. The Color Doppler maps were segmented using the Power Doppler data and overlaid onto the high-quality B-mode shown in figure 2(*c*) and acquired immediately after the 1 s one-source acquisition sequence at 3000 volumes s^{-1}. The Tissue Doppler was overlaid onto the B-mode images and segmented by applying a dilation operation onto the Power Doppler mask. The

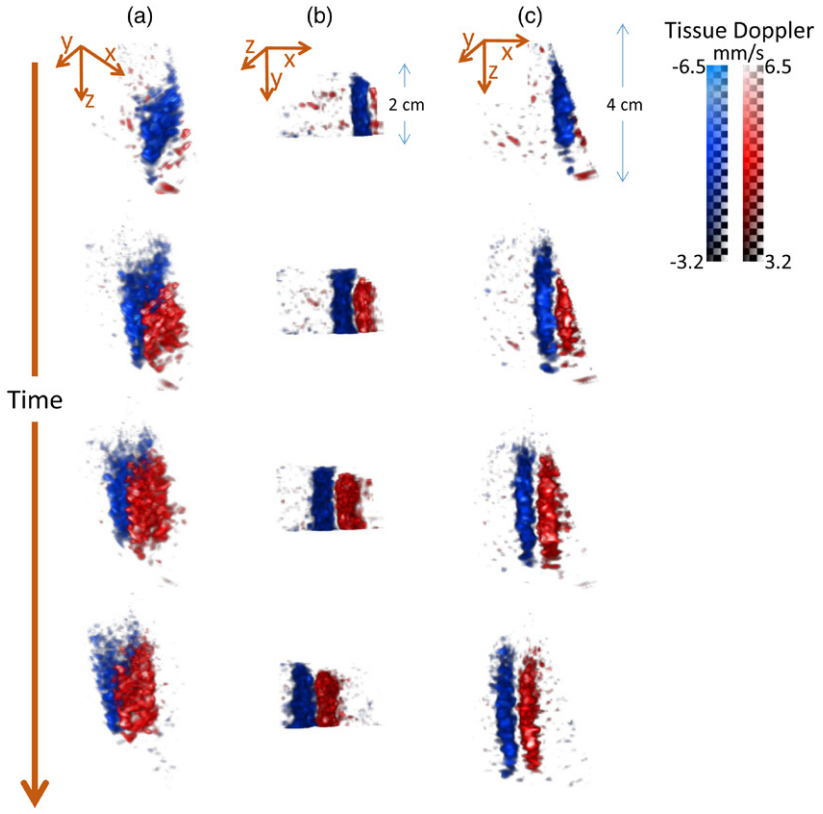

Figure 3. Motion estimation for 3D shear-wave imaging. Propagation of a shear-wave generated using radiation force from an (*a*) approximately isometric view, from (*b*) a top view and (*c*) a side view. The velocity of the wave was found to be approximately 0.8 m s^{-1} and corresponds to the stiffness of the phantom used (1.92 kPa).

bifurcation of the carotid could be identified and fully characterized as it was visible in both the high-quality B-mode and the Ultrafast Doppler Imaging ciné-loop. For instance, one can observe the Power Doppler Spectrum in any voxel, including at the entrance and exits of the bifurcation (figure 5). Figure 5 also shows the propagation of the pulse wave in the carotid wall (Couade *et al* 2010, Luo *et al* 2012); which is a flow velocity, pressure, and diameter waves generated at the ejection phase of the left ventricle (Nichols *et al* 2011).

3. Discussion

In this study, we have demonstrated the feasibility of 3D Ultrafast Ultrasound Imaging in humans *in vivo*. More specifically, we have shown that by using a virtual array located behind the probe, it is possible to achieve high contrast and good resolution with a small number of coherently compounded emissions, hence allowing for the imaging of thousands of volumes per second. Such high volume rates allow, in turn, for the accurate mapping in entire 3D volumes of Color Doppler, Power Doppler, Pulsed Doppler, and Tissue Doppler of each individual voxel. By implementing each algorithm on GPUs, it was shown possible to obtain these

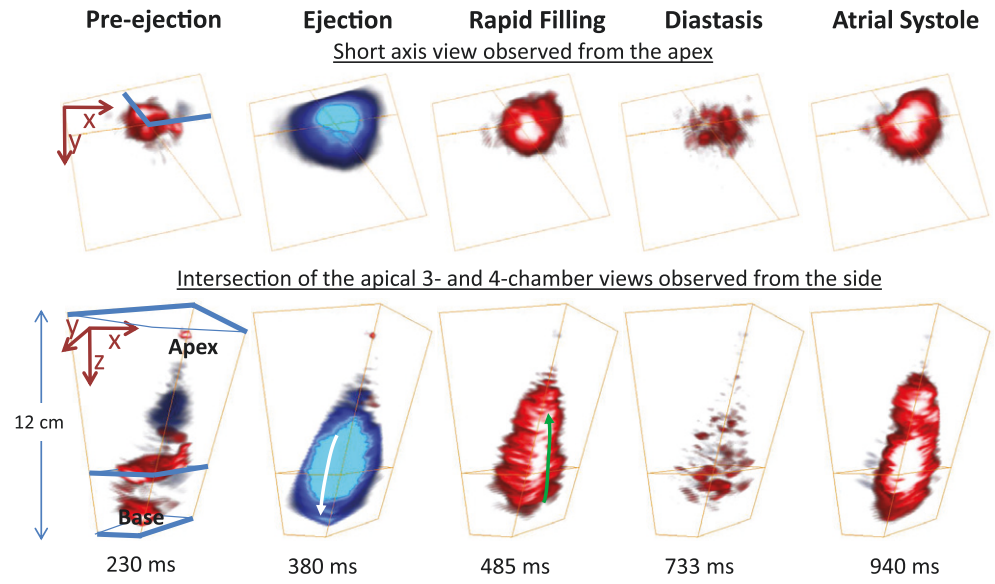

Figure 4. 3D Ultrafast Doppler Imaging in the heart. Blood flow in the left ventricle of a healthy volunteer during an entire cardiac cycle. After segmentation using the Power Doppler data, different well-known phases can be identified in the Color Flow Doppler ciné-loops, such as ejection and rapid filling.

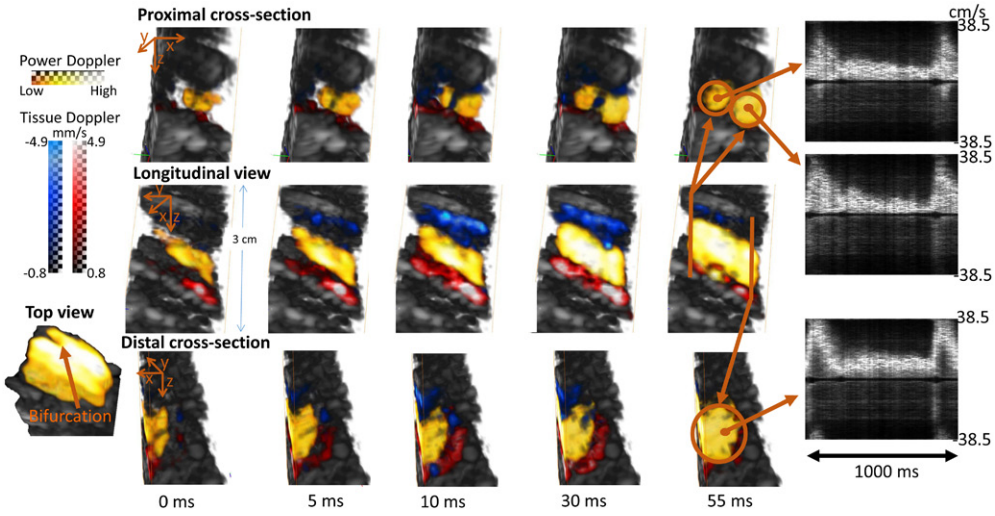

Figure 5. 3D Ultrafast Doppler Imaging of the carotid bifurcation. Blood flow and tissue motion in the bifurcation of the carotid artery of a healthy volunteer overlaid onto a high quality B-mode volume during an entire cardiac cycle, along with quantitative blood flow shown for three regions at the entrance and exit of the bifurcation. The top view, which was cropped to the center of the carotid artery, can be used to clearly identify the location of the bifurcation.

quantities in real-time or in a few seconds following acquisition depending on the required imaging depth and spatial sampling.

Figure 2 (supplementary video 1 (stacks.iop.org/PMB/59/00L1/mmedia)) demonstrated that coherent compounding can be used to achieve an optimal, application-dependent trade-off between contrast, resolution, and volume rate. Figure 3 (supplementary video 2 (stacks.iop.org/PMB/59/00L1/mmedia)) demonstrated the feasibility of both 3D Tissue Doppler and Shear-Wave Imaging for the mechanical characterization of tissues in 3D. Figure 4 (supplementary video 3 (stacks.iop.org/PMB/59/00L1/mmedia)) demonstrated the feasibility of Ultrafast Doppler Imaging can be performed in the challenging clinical setting of cardiac imaging in which we were able to fully characterize all the phases of the cardiac cycle. Finally, figure 5 (supplementary video 4 (stacks.iop.org/PMB/59/00L1/mmedia)) shows that 3D Ultrafast Doppler Imaging and 3D Tissue Doppler Imaging can be performed in the carotid in a single acquisition and overlaid onto a high-quality B-mode obtained at approximately 100 volumes s^{-1}, which is more than sufficient for anatomical imaging.

3D Ultrafast Ultrasound Imaging could potentially revolutionize current clinical practices. Indeed, we have shown that by using 3D Ultrafast Ultrasound Imaging, blood flow can be visualized and quantified, e.g. in the totality of the carotid bifurcation, in order to identify the presence of abnormalities. Perhaps more importantly, the techniques detailed herein can be applied, theoretically, to any other organ. In the heart, a single 3D Ultrafast Ultrasound Imaging acquisition could provide 1) the 3D anatomy of all four cardiac chambers to measure standard quantities, such as the wall motion in all wall segments and the ejection fraction; 2) the quantitative blood flow, i.e. both pulsed and color Doppler, in each individual voxel of the volume to assess, e.g. all four valves' functions simultaneously and their relationships in the presence of obstacles or shunts in congenital cardiomyopathy; and 3) the cardiac displacement and strains in the entire heart both in their clinical form, e.g. peak systolic strains in all segments, or in novel versions requiring high frame rates, which can be used, e.g. to map the electromechanical activation sequence of the heart (Provost *et al* 2011a) or to locate ischemic regions (Lee *et al* 2011). Additionally, 3D Ultrafast Ultrasound Imaging could potentially complement or enhance existing techniques to image blood flow in 3D, such as magnetic resonance phase contrast velocimetry (Caroff *et al* 2012) or echocardiographic particle imaging velocimetry (Sengupta *et al* 2012), since it is portable and does not require ECG-gating or the injection of contrast agents. Additionally, in the presence of such contrast agents, since 3D Ultrafast Ultrasound Imaging is based on diverging emissions, it could further improve image quality both in terms of resolution (Desailly *et al* 2013) and contrast (Couture *et al* 2009, 2012).

Limitations to the technique include the reduced energy transmitted to the tissues, especially when a large field of view is needed, as it requires the use of spherical waves emerging from virtual sources located close to the probe. Indeed, the ultrasound pulse energy decreases as the square of the depth, without taking into account attenuation. This limitation can, however, be overcome by using the coherent compounding of multiple emissions, coded excitations, pre-amplified probes, or the development of higher-powered pulsers. Indeed, using compounded diverging waves allows for the safe propagation of large cumulative energy while ensuring limited tissue heating and small instantaneous local pressure, both of which are at the source of known potential adverse bioeffects. Moreover, the results of the resolution experiment of figure 2(*a*) are to be considered only qualitatively, as the metallic beads used were not sufficiently small against the focal zone size to provide quantitative resolution results; a complete quantitative resolution study is the object of on-going work.

Another important feature of 3D Ultrafast Imaging is the simultaneous acquisition of all radiofrequency element data within the observation volume. Such simultaneous and large field of view acquisitions can be used to improve image quality in post-processing, e.g. by allowing for the implementation of aberration correction techniques, which are currently known to be of limited interest in 2D as they do not account for out-of-plane aberrations. Moreover, motion compensation algorithms, for example in cardiac applications, as recently demonstrated in 2D (Denarie *et al* 2013), could be extended to 3D ultrafast acquisitions.

In conclusion, we have demonstrated the feasibility of 3D Ultrasound Ultrafast Imaging in humans *in vivo* is a novel approach for the simultaneous quantitative, functional, and anatomical imaging of tissues in 3D at very high volume rates. Such a technology allows for the mapping of blood flow and tissue motion in entire 3D fields of view and promises to enhance the current limitations of 2D echography in terms of inter—and intra-observer variability and to generate a host of novel 3D applications ranging from brain activation mapping and cardiac electrophysiology to ultrasound-based angiography and 3D Shear-Wave Imaging of tumors.

Acknowledgements

This work was supported by the European Research Council under the European Union's Seventh Framework Programme (FP/2007–2013) / ERC Grant Agreement n°311025 and by LABEX WIFI (Laboratory of Excellence ANR-10-LABX-24) within the French Program 'Investments for the Future' under reference ANR-10-IDEX-0001-02 PSL. J P is funded by a Marie Curie International Incoming Fellowship.

References

Bercoff J, Tanter M and Fink M 2004 Supersonic shear imaging: a new technique for soft tissue elasticity mapping *IEEE Trans. Ultrason. Ferroelectr. Freq. Control* **51** 396–409

Caroff J, Bière L, Trebuchet G, Nedelcu C, Sibileau E, Beregi J-P, Aubé C, Furber A and Willoteaux S 2012 Applications of phase-contrast velocimetry sequences in cardiovascular imaging *Diagn. Interv. Imag.* **93** 159–70

Couade M, Pernot M, Prada C, Messas E, Emmerich J, Bruneval P, Criton A, Fink M, and Tanter M 2010 Quantitative assessment of arterial wall biomechanical properties using shear wave imaging *Ultrasound Med. Biol.* **36** 1662–76

Couade M, Pernot M, Tanter M, Messas E, Bel A, Ba M, Hagege A-A, and Fink M 2009 Ultrafast imaging of the heart using circular wave synthetic imaging with phased arrays *Ultrasonics Symposium (IUS), 2009 IEEE International. Presented at the Ultrasonics Symposium (IUS), 2009 IEEE International* pp 515–8

Couture O, Bannouf S, Montaldo G, Aubry J-F, Fink M and Tanter M 2009 Ultrafast imaging of ultrasound contrast agents *Ultrasound Med. Biol.* **35** 1908–16

Couture O, Fink M and Tanter M 2012 Ultrasound contrast plane wave imaging *IEEE Trans. Ultrason. Ferroelectr. Freq. Control* **59** 2676–83

Demené C, Pernot M, Biran V, Alison M, Fink M, Baud O and Tanter M 2014 Ultrafast Doppler reveals the mapping of cerebral vascular resistivity in neonates *J. Cereb. Blood Flow Metab.* **34** 1009–17

Denarie B, Bjastad T and Torp H 2013 Multi-line transmission in 3D with reduced crosstalk artifacts: a proof of concept study *IEEE Trans. Ultrason. Ferroelectr. Freq. Control* **60** 1708–18

Desailly Y, Couture O, Fink M and Tanter M 2013 Sono-activated ultrasound localization microscopy *Appl. Phys. Lett.* **103** 174107

Dort S, Muth S, Swillens A, Segers P, Cloutier G and Garcia D 2012 Vector flow mapping using plane wave ultrasound imaging *Ultrasonics Symposium (IUS), 2012 IEEE International. Presented at the Ultrasonics Symposium (IUS), 2012 IEEE International* pp 330–3

Ekroll I K, Swillens A, Segers P, Dahl T, Torp H and Lovstakken L 2013 Simultaneous quantification of flow and tissue velocities based on multi-angle plane wave imaging *IEEE Trans. Ultrason. Ferroelectr. Freq. Control* **60** 727–38

Fink M and Tanter M 2010 Multiwave imaging and super resolution *Phys. Today* **63** 28–33

Fujikura K, Luo J, Gamarnik V, Pernot M, Fukumoto R, Tilson M D and Konofagou E E 2007 A novel noninvasive technique for pulse-wave imaging and characterization of clinically-significant vascular mechanical properties *in vivo Ultrason. Imag.* **29** 137–54

Hazard C R and Lockwood G R 1999 Theoretical assessment of a synthetic aperture beamformer for real-time 3D imaging *IEEE Trans. Ultrason. Ferroelectr. Freq. Control* **46** 972–80

Honjo Y, Hasegawa H and Kanai H 2010 2D tracking of heart wall for detailed analysis of heart function at high temporal and spatial resolutions *Jpn. J. Appl. Phys.* **49** 07HF14

Kasai C, Namekawa K, Koyano A and Omoto R 1985 Real-time 2D blood flow imaging using an autocorrelation technique *IEEE Trans. Sonics Ultrason.* **32** 458–64

Konofagou E, Lee W-N, Luo J, Provost J and Vappou J 2011 Physiologic cardiovascular strain and intrinsic wave imaging *Annu. Rev. Biomed. Eng.* **13** 477–505

Lee W-N, Pernot M, Couade M, Messas E, Bruneval P, Bel A, Hagege A A, Fink M and Tanter M 2012 Mapping myocardial fiber orientation using echocardiography-based shear wave imaging *IEEE Trans. Med. Imag.* **31** 554–62

Lee W-N, Provost J, Fujikura K, Wang J and Konofagou E E 2011 *In vivo* study of myocardial elastography under graded ischemia conditions *Phys. Med. Biol.* **56** 1155–72

Lockwood G R, Talman J R and Brunke S S 1998 Real-time 3D ultrasound imaging using sparse synthetic aperture beamforming *IEEE Trans. Ultrason. Ferroelectr. Freq. Control* **45** 980–8

Luo J, Li R X and Konofagou E E 2012 Pulse wave imaging of the human carotid artery: an *in vivo* feasibility study *IEEE Trans. Ultrason. Ferroelectr. Freq. Control* **59** 174–81

Macé E, Montaldo G, Cohen I, Baulac M, Fink M and Tanter M 2011 Functional ultrasound imaging of the brain *Nat. Methods* **8** 662–4

Montaldo G, Tanter M, Bercoff J, Benech N and Fink M 2009 Coherent plane-wave compounding for very high frame rate ultrasonography and transient elastography *IEEE Trans. Ultrason. Ferroelectr. Freq. Control* **56** 489–506

Nichols W, O'Rourke M and Vlachopoulos C 2011 *McDonald's Blood Flow in Arteries, Sixth Edition: Theoretical, Experimental and Clinical Principles* 6th edn (London: CRC)

Nikolov S I 2001 *Synthetic Aperture Tissue and Flow Ultrasound Imaging* (Lyngby: Orsted-DTU, Technical University of Denmark)

Nikolov S I, Kortbek J and Jensen J A 2010 Practical applications of synthetic aperture imaging *2010 IEEE Ultrasonics Symposium (IUS). Presented at the 2010 IEEE Ultrasonics Symposium (IUS)* pp 350–8

Osmanski B F, Martin C, Montaldo G, Lanièce P, Pain F, Tanter M and Gurden H 2014 Functional ultrasound imaging reveals different odor-evoked patterns of vascular activity in the main olfactory bulb and the anterior piriform cortex *NeuroImage* **95** 176–84

Osmanski B F, Maresca D, Messas E, Tanter M and Pernot M 2014 Transthoracic ultrafast Doppler imaging of human left ventricular hemodynamic function *IEEE Trans. Ultrason. Ferroelectr. Freq. Control* **61** 1268–75

Papadacci C, Pernot M, Couade M, Fink M and Tanter M 2014 High-contrast ultrafast imaging of the heart *IEEE Trans. Ultrason. Ferroelectr. Freq. Control* **61** 288–301

Papadacci C, Tanter M, Pernot M and Fink M 2014 Ultrasound backscatter tensor imaging (BTI): analysis of the spatial coherence of ultrasonic speckle in anisotropic soft tissues *IEEE Trans. Ultrason. Ferroelectr. Freq. Control* **61** 986–96

Pernot M, Fujikura K, Fung-Kee-Fung S D and Konofagou E E 2007 ECG-gated, mechanical and electromechanical wave imaging of cardiovascular tissues *in vivo Ultrasound Med. Biol.* **33** 1075–85

Perrin D P, Vasilyev N V, Marx G R and del Nido P J 2012 Temporal enhancement of 3D echocardiography by frame reordering *JACC Cardiovasc. Imaging* **5** 300–4

Provost J, Gambhir A, Vest J, Garan H and Konofagou E E 2013 A clinical feasibility study of atrial and ventricular electromechanical wave imaging *Heart Rhythm* **10** 856–62

Provost J, Lee W-N, Fujikura K and Konofagou E E 2010 Electromechanical wave imaging of normal and ischemic hearts *in vivo IEEE Trans. Med. Imaging* **29** 625–35

Provost J, Lee W-N, Fujikura K and Konofagou E E 2011a Imaging the electromechanical activity of the heart *in vivo Proc. Natl. Acad. Sci.* **108** 8565–70

Provost J, Nguyen V T-H, Legrand D, Okrasinski S, Costet A, Gambhir A, Garan H and Konofagou E E 2011b Electromechanical wave imaging for arrhythmias *Phys. Med. Biol.* **56** L1–11

Provost J, Thiébaut S, Luo J and Konofagou E E 2012 Single-heartbeat electromechanical wave imaging with optimal strain estimation using temporally-unequispaced acquisition sequences *Phys. Med. Biol.* **57** 1095–112

Sandrin L, Catheline S, Tanter M, Hennequin X and Fink M 1999 Time-resolved pulsed elastography with ultrafast ultrasonic imaging *Ultrason. Imag.* **21** 259–72

Sandrin L *et al* 2003 Transient elastography: a new noninvasive method for assessment of hepatic fibrosis *Ultrasound Med. Biol.* **29** 1705–13

Sengupta P P, Pedrizetti G and Narula J 2012 Multiplanar visualization of blood flow using echocardiographic particle imaging velocimetry *JACC Cardiovasc. Imag.* **5** 566–9

Skaug T R, Amundsen B H, Hergum T, Urheim S, Torp H and Haugen B O 2013 Quantification of aortic regurgitation using high-pulse repetition frequency 3D colour Doppler *Eur. Heart J. Cardiovasc. Imag.* **15** 615–22

Tanter M, Bercoff J, Athanasiou A, Deffieux T, Gennisson J-L, Montaldo G, Muller M, Tardivon A and Fink M 2008 Quantitative assessment of breast lesion viscoelasticity: initial clinical results using supersonic shear imaging *Ultrasound Med. Biol.* **34** 1373–86

Tanter M, Bercoff J, Sandrin L and Fink M 2002 Ultrafast compound imaging for 2D motion vector estimation: application to transient elastography *IEEE Trans. Ultrason. Ferroelectr. Freq. Control* **49** 1363–74

Tanter M and Fink M 2014 Ultrafast imaging in biomedical ultrasound *IEEE Trans. Ultrason. Ferroelectr. Freq. Control* **61** 102–19

Udesen J, Gran F, Hansen K L, Jensen J A, Thomsen C and Nielsen M B 2008 High frame-rate blood vector velocity imaging using plane waves: simulations and preliminary experiments *IEEE Trans. Ultrason. Ferroelectr. Freq. Control* **55** 1729–43

Vappou J, Luo J and Konofagou E E 2010 Pulse wave imaging for noninvasive and quantitative measurement of arterial stiffness *in vivo Am. J. Hypertens.* **23** 393–8

Wang S, Lee W-N, Provost J, Luo J and Konofagou E E 2008 A composite high-frame-rate system for clinical cardiovascular imaging *IEEE Trans. Ultrason. Ferroelectr. Freq. Control* **55** 2221–33

Yiu B, Lai S and Yu A 2014 Vector projectile imaging: time-resolved dynamic visualization of complex flow patterns *Ultrasound Med. Biol.* **40** 2295–309